

Origin of spin gap in CaV_4O_9 : effect of frustration and lattice distortion

O. A. Starykh¹, M. E. Zhitomirsky², D. I. Khomskii³, R. R. P. Singh¹, and K. Ueda²

¹*Department of Physics, University of California, Davis, California 95616*

²*Institute for Solid State Physics, University of Tokyo, Tokyo 106, Japan*

³*Groningen University, 9747 AG Groningen, The Netherlands*

(today)

We study the origin of spin-gap in recently discovered material CaV_4O_9 . We analyze the spin-1/2 Heisenberg model on the 1/5 depleted square lattice with nearest neighbor (nn) and next nearest neighbor (nnn) interactions, in terms of the singlet and triplet states of the 4-spin plaquettes and 2-spin dimers. Phase diagram of the model is obtained within a linear “spin-wave”-like approximation, and is shown to agree well with the earlier results of QMC simulations for nn interactions. We further propose that the special lattice structure of CaV_4O_9 naturally leads to lattice distortions, which enhances the spin-gap via a spin-Peierls mechanism.

PACS: 75.10.Jm, 75.30.Kz, 75.40.Cx, 75.50.Ee

Recent discovery [1] of a quantum disordered phase and spin-gap in the layered magnet CaV_4O_9 has attracted considerable interest [2,3,4,5,6]. The magnetic system can be described by a Heisenberg model for spins of Vanadium ions ($S = 1/2$) on a 1/5-depleted square lattice. At each site of this bipartite lattice three bonds meet: two of them belong to the 4-spin plaquettes covering the lattice (plaquette bonds), whereas the third one (dimer bond) connects a plaquette with its neighbor (see Fig. 1). Since the coupling between spins is mediated by superexchange via intermediate Oxygens, a strong next nearest neighbor interaction is also expected [2,4].

We are thus led to the following Hamiltonian:

$$\hat{H} = \sum_{\text{n.n.}} J_{nn} \mathbf{S}_i \cdot \mathbf{S}_j + J_2 \sum_{\text{n.n.n.}} \mathbf{S}_i \cdot \mathbf{S}_j, \quad (1)$$

where the nn interaction J_{nn} equals J_0 (J_1) for plaquette (dimer) bond. It is evident that this model has disordered singlet ground states in two limits: for $J_0 \gg J_1, J_2$ the ground state is a product of singlets on each plaquette, and for $J_1 \gg J_0, J_2$ it consists of singlets on the dimers. However, a physically relevant choice of exchange parameters is $J_0 \approx J_1$.

For model (1) a spin-gap can arise either from the non-equivalence of the dimer and plaquette bonds ($J_0 \neq J_1$), or from the effects of frustration due to nnn couplings. Previous theoretical works have mainly focused on the former. Quantum Monte Carlo (QMC) simulations, done with $J_2 = 0$ [6], show that the 1/5-depleted square lattice has Neel order for $J_0 = J_1$. However, the system is close to the transition into the disordered phase.

The aim of this paper is twofold. First, we describe an efficient analytical approach to study the $T = 0$ phase

diagram of (1) in the $J_1/J_0 - J_2/J_0$ plane, and show that a moderate $J_2 \sim 0.2J_0$, with $J_1 = J_0$, can account for the experimental data. Second, we point out that the special lattice structure of this system inevitably leads to lattice distortions, resulting in the strengthening of the Plaquette bonds with respect to the Dimers. Thus the spin-Peierls mechanism cooperates with the intrinsic tendencies of the system in forming a spin-gap.

The phase diagram of the Hamiltonian (1) for $J_2 = 0$ has been studied analytically using linear spin-wave [2], strong coupling perturbation [2,3], mean-field Schwinger boson [5] and cluster [2] approaches. As expected, both spin-wave and Schwinger boson theories substantially overestimate the region of stability of the Néel phase compared to QMC data [6], while expansions around strong-coupling limits favor disordered phases. Here, we investigate this model using bosonization techniques which correctly account for short-range spin correlations inside the plaquette and dimer blocks.

For the closely related case of the frustrated square-lattice antiferromagnet the disordered spin-state is a dimer state, formation of which is accompanied by a spontaneous breaking of the lattice symmetry [7,8]. In contrast, for the CaV_4O_9 -lattice the choice of spins which form singlets is determined by the structure of the lattice and there is no spontaneous symmetry breaking. However, two different types of disordered short-range RVB states, with spin-singlets formed on plaquettes and dimers, are possible [2,3]. For different values of model parameters one needs to consider representations for spin operators in terms of both dimer and plaquette states. We generalize previous derivations of such representations [7,9,10,11] for the two cases.

The starting point of these representations are non-interacting spin blocks. Let states of a single block be given by $|\alpha\rangle$. In case of dimers, they are a singlet $|s\rangle$ ($E_s = -\frac{3}{4}J_1$) and a triplet $|t_\alpha\rangle$, $\alpha = x, y$, and z ($E_t = \frac{1}{4}J_1$). All 16 states of a four spin plaquette can be found in Ref. [2,9]. The lowest levels, once again, are a singlet with energy $E_s = -2J_0 + \frac{1}{2}J_2$, and a triplet with $E_t = -J_0 + \frac{1}{2}J_2$. In the bosonic representation for plaquette spins we will restrict ourselves to these four states only. This assumes that occupation numbers of all higher levels are small.

The site spins \mathbf{S}_i are expressed in terms of the basis block states as

$$\mathbf{S}_i = \langle \alpha | \mathbf{S}_i | \beta \rangle Z^{\alpha\beta}, \quad (2)$$

where $Z^{\alpha\beta}$ is the projection operator $|\alpha\rangle\langle\beta|$ and summation over repeated indices is assumed.

Consider first the matrix elements that occur in Eq.(2), in the subspace of one singlet and three triplet states. Using rotational invariance in spin space and time-reversal symmetry one gets

$$\begin{aligned} \langle s | \mathbf{S}_i^\alpha | s \rangle &= 0, \quad \langle s | \mathbf{S}_i^\alpha | t_\beta \rangle = \delta_{\alpha\beta} A_{st}^i, \\ \langle t_\alpha | \mathbf{S}_i^\beta | t_\gamma \rangle &= i e^{\alpha\beta\gamma} A_{tt}^i, \end{aligned} \quad (3)$$

where $e^{\alpha\beta\gamma}$ is the totally antisymmetric tensor and A_{st}^i , A_{tt}^i are real. Let each spin of the block be decomposed as $\mathbf{S}_i = \mathbf{L}_i + \mathbf{M}_i$, where \mathbf{L}_i has nonzero matrix elements between triplets and singlet, while \mathbf{M}_i acts between triplets only. It is easy to see that \mathbf{M}_i must be proportional to the total spin of the block, and, thus, is independent of i , whereas $\mathbf{L}_i \propto (-1)^i$ for blocks consisting of equivalent spins. Further calculations using explicit forms of singlet and triplet states are straightforward and give $A_{st}^i = (-1)^i/2$, $A_{tt}^i = 1/2$ for dimers, and $A_{st}^i = (-1)^i/\sqrt{6}$, $A_{tt}^i = 1/4$ for plaquettes.

We define the vacuum $|0\rangle$ and four boson operators that yield the four physical states $|s\rangle = s^+|0\rangle$, $|t_\alpha\rangle = t_\alpha^+|0\rangle$. The projection operators are naturally expressed as $Z^{st_\alpha} = s^+t_\alpha$, $Z^{t_\alpha t_\beta} = t_\alpha^+t_\beta$, and so on. Block spins represented via these boson operators are

$$\begin{aligned} S_i^\alpha &= \frac{(-1)^i}{2}(s^+t_\alpha + t_\alpha^+s) - \frac{i}{2}e^{\alpha\beta\gamma}t_\beta^+t_\gamma, \quad \text{for dimers,} \\ S_i^\alpha &= \frac{(-1)^i}{\sqrt{6}}(s^+t_\alpha + t_\alpha^+s) - \frac{i}{4}e^{\alpha\beta\gamma}t_\beta^+t_\gamma, \quad \text{for plaquettes.} \end{aligned} \quad (4)$$

Commutation relations between spins are satisfied as long as bosonic representation preserves the algebra of the projection operators, i.e. the relation $Z^{\alpha\beta}Z^{\alpha'\beta'} = \delta_{\alpha'\beta}Z^{\alpha\beta'}$. This requirement restricts the number of bosons allowed on each block to one:

$$s^+s + t_\alpha^+t_\alpha = 1. \quad (5)$$

With the help of this constraint the Hamiltonian of a single block becomes $\hat{H}_B = E_s s^+s + E_i t_\alpha^+t_\alpha$. There are two ways to implement the constraint (5). First is the slave-boson treatment of Sachdev and Bhatt [7], where relation (5) is imposed by a Lagrange multiplier. The second approach [11] is to express the s -operators in terms of the t_α -operators

$$s^+ = s = \sqrt{1 - t_\alpha^+t_\alpha}, \quad (6)$$

and substitute into Eq. (4). Instead of the Holstein-Primakoff type representation (6), we can also consider an analog of the nonhermitian Dyson-Maleev representation: $s^+ = 1$ and $s = 1 - t_\alpha^+t_\alpha$ [10]. Note that the block Hamiltonian is treated identically in both approaches. Differences appear when interactions between the blocks are switched on.

As in case of spin-wave theory for ordered magnetic phases, one might expect even the linear approximation, which neglects interaction between excitations, to work well. This approximation can be formulated for both types of block spin representations in the same way. It consists of replacing s and s^+ by 1, when calculating $(\mathbf{S}_i \cdot \mathbf{S}_j)$ for pairs of spins from different blocks. Also, only terms of second order in triplet operators should be kept. Diagonalization of the resulting quadratic form is done by a standard Bogoliubov transformation, and one finds a 3-fold degenerate spectrum of triplet excitations. For small coupling between the blocks the spectrum is positive with a gap. Increasing the interaction between the blocks decreases the gap, which finally vanishes at the transition between disordered and ordered phases.

First, consider the plaquette singlet phase which exists for large J_0 . The spectrum of spin-1 excitations is threefold degenerate and has the dispersion

$$\omega_p^2(\mathbf{k}) = J_0 \left[J_0 + \frac{2}{3}(J_1 - 2J_2)(\cos k_x + \cos k_y) \right]. \quad (7)$$

The minimum of the spectrum is at (π, π) for $(J_1 - 2J_2) > 0$ and at $(0, 0)$ for $(J_1 - 2J_2) < 0$. From Eq. (7) one finds the region of stability of the plaquette phase, shown in Fig. 2. At $J_2 = 0$, singlets on 4-spin plaquettes become unstable at the critical ratio $J_0/J_1|_{\text{cr}} = \frac{4}{3}$, which is not too far from the QMC estimate $J_0/J_1|_{\text{cr}} = 1.1$ [6]. The total energy of this phase, per spin, is

$$E_{\text{g.s.}}^p = -\frac{1}{2}J_0 + \frac{1}{8}J_2 + \frac{3}{8N} \sum_{\mathbf{k}} [\omega_p(\mathbf{k}) - J_0]. \quad (8)$$

It consists of the energy of noninteracting plaquette singlets and the energy of zero-point fluctuations.

In the dimer state each crystal unit cell has two dimers. Therefore, there are two different branches of $S = 1$ magnons in the Brillouin zone. However, calculations are greatly simplified if instead we consider only one type of dimers, which are defined in the new Brillouin zone corresponding to the lattice formed by the centers of dimer bonds. This procedure is quite similar to performing a spin-wave expansion around the rotating quantization axis, as is often done in standard spin-wave theory. As a result, we obtain one triply degenerate excitation mode in the new Brillouin zone, which is twice the original one,

$$\begin{aligned} \omega_d^2(\mathbf{k}) &= J_1 [J_1 - (J_0 - J_2)(\cos k_x - \cos k_y) \\ &\quad - J_2 \cos(k_x + k_y)]. \end{aligned} \quad (9)$$

The minimum of the spectrum is at $\mathbf{k} = (0, \pi)$ for $J_2 < \frac{1}{3}J_0$, and moves into the interior of the zone for larger J_2 . At $J_2 = 0$, the dimer phase is unstable for $J_0/J_1 > \frac{1}{2}$, while the corresponding critical ratio from QMC is $J_0/J_1|_{\text{cr}} = 0.6 \pm 0.05$ [6]. Note that the instabilities of the Néel phase at $J_2 = 0$, as predicted by our linear bosonic theory, coincide with the mean field cluster approach [2]. However, the latter is not appropriate

to study spin-liquid phases. The total energy per spin in the dimer phase is

$$E_{\text{g.s.}}^d = -\frac{3}{8}J_1 + \frac{3}{4N} \sum_{\mathbf{k}} [\omega_d(\mathbf{k}) - J_1] . \quad (10)$$

Phase diagram of the model (1) follows from Eqs. (7) and (9). When frustration exceeds the critical value $J_2^{\text{cr}} = 0.25J_0$, the Néel phase ceases to exist. A first order transition line separates plaquette and dimer phases since their symmetries are different [2]. This line is found by comparing (8) and (10) and is shown in Fig. 2 [12].

As J_2 grows, the energies of the omitted plaquette states decrease making the linear approximation less satisfactory, and at $J_2 = J_0$ the second singlet which consists of two crossing dimers becomes the ground state of the 4-spin plaquette [2,9]. We have checked that this phase is not stable in the linear approximation for any values of the parameters. Another possible short-range RVB state is the plaquette-RVB on large squares formed by J_2 bonds, but it was also found to be unstable. Therefore, for large values of J_2 magnetic order should be stabilized again. It is easy to see that in the limit $J_2 \gg J_0, J_1$ spins are arranged into two interpenetrating Néel ordered sublattices which are decoupled at the classical level. The degeneracy with respect to a relative orientation of antiferromagnetic vectors should be removed by quantum fluctuations, providing an example of ‘order-from-disorder’ phenomenon [13]. We have presented in Fig. 2 transition line between this ordered state and disordered plaquette phase.

A theoretical comment is in order here. Calculations described above can be repeated within an alternative slave-boson treatment [7], which amounts to introducing a singlet condensate $\bar{s}^2 \neq 1$ and a chemical potential μ , and finding their values self-consistently. Solving the self-consistent equations for the phase boundaries, we found, at $J_2 = 0$, that dimer phase is stable for $J_0/J_1 \leq 0.874$, whereas plaquette-RVB exists up to $J_0/J_1 = 0.76$. Thus, unlike linear approximation, mean-field slave-boson treatment predicts *no* ordered phase even at $J_2 = 0$, in striking contradiction with numerical simulations and linear approximation results. Situation is not improved even upon taking triplet-triplet interaction into account - its effect on the location of phase boundaries is ridiculously small, less than 1 per cent. These findings clearly favor our linear approximation as the most suitable one for the problem at hand.

To make contact with experiments, let us first confine ourselves to $J_0 = J_1$. Note that only second terms of Eq. (4) contribute to the uniform susceptibility, leading to $\chi \sim \frac{1}{TN} \sum_{\mathbf{k}} n(\omega_{\mathbf{k}})(1 + n(\omega_{\mathbf{k}}))$, where $n(\omega)$ is the Bose factor. We can compare the Curie-Weiss relation $\theta = \frac{3}{4}(J_0 + J_2)$ and the gap Δ , in Eq. (7) appropriate for the PRVB phase, with the experimental Curie Weiss constant and the gap determined from the T-dependence of the

susceptibility. We find that the experimental numbers $\Delta = 107$ K and $\theta = 220$ K [1] can arise from two sets of exchange constants (i) $J_0 = 245$ K, $J_2 = 48$ K and (ii) $J_0 = 193$ K, $J_2 = 100$ K. Thus this theory, by itself, can provide a consistent description of the properties of CaV_4O_9 observed so far.

However, we would now like to point out an additional aspect of this material which has so far gone unnoticed. Because of the special lattice structure, spin-phonon couplings will cause a gain in magnetic energy which is **linear** in the lattice distortion, whereas the loss in elastic energy is always quadratic. Thus there will always be a lattice distortion in this system which will cause the plaquette bonds to shrink and the dimer bonds to elongate. This will lead to $J_0 > J_1$. This spin-Peierls mechanism will enhance the stability of the PRVB phase and contribute to the spin-gap.

To get a quantitative estimate, let the shrinking of the plaquettes change the distance between the Vanadium ions from R to $R \pm 2u$. Using the phenomenological relation $J(R) \approx \text{const}/R^{10}$ [14], the exchange constants J_0 (J_1) increase (decrease) by $\delta J = 20uJ/R$. The magnetic energy gain per Vanadium atom is $e_m = -\delta J(C_1 - 0.5C_2)$, where C_1 and C_2 are spin correlations on the plaquette and dimer bonds in the absence of distortion. It is sufficient to evaluate them on the Neel state, where they both are $-1/4$. Thus the gain in magnetic energy per unit volume is $E_m \sim (20uJ/8R)(1/R^2R_{\perp})$, where R_{\perp} is the distance between magnetic layers. A rough estimate for the elastic energy per unit volume is $E_{\text{ph}} \sim \frac{1}{2}B(u/R)^2$, where B is a bulk modulus of the material. Minimizing the energies leads to a distortion $u \sim (5J/2BR_{\perp})$, which induces a variation of the exchange integrals by

$$\delta J/J \approx (50J/R^2R_{\perp}B). \quad (11)$$

Taking $R = 3 \text{ \AA}$, $R_{\perp} = 5 \text{ \AA}$, $J = 300$ K, $B = 10^{12}$ dynes/cm², we get $u/R \sim 10^{-3}$ and $\delta J/J \sim 10^{-2} - 10^{-1}$. These values are similar to what is found in most of the spin-Peierls materials [15], where $J_0/J_1 \sim 1.3$. This similarity is not unexpected as the linear gain in magnetic energy is somewhat analogous to $u^{4/3}$ gain in a 1D spin- $\frac{1}{2}$ chain [16].

If J_2 was negligible, and the spin-Peierls mechanism was entirely responsible for the spin-gap, we would use Eq. (7) with $J_2 = 0$ and the Curie-Weiss relation $\theta = \frac{1}{4}(2J_0 + J_1)$ to compare with experiments. This leads to estimates $J_0 = 331$ K, $J_1 = 218$ K. The ratio $J_0/J_1 \sim 1.5$ corresponds to $\delta J = 0.2J$, which is somewhat larger than our earlier back of the envelop estimate, suggesting that some J_2 is needed to explain the data.

We note that here the spin-Peierls mechanism does not lead to a spontaneous breaking of the lattice symmetry. Hence, we do not expect a sharp change in the lattice distortion u with temperature. Instead, it

should follow short-range order and the spin-gap should be temperature-dependent. Finally, we point out that most known spin-Peierls materials have first order structural phase transition at high temperature [15]. This creates a soft phonon mode in the system, which in the end favors the spin-Peierls phenomena [17]. Curiously enough, a small discontinuous jump in $\chi(T)$ at 340 K was observed also in CaV_4O_9 [1], but was attributed to an admixture of the VO_2 phase. In view of our proposal this point should be studied more carefully.

Our discussion of possible spin-Peierls phenomena is only an order of magnitude estimate. Nevertheless it shows that spin-phonon coupling may successfully “co-operate” with intrinsic tendencies for forming a spin-gap due to the frustrating next-nearest-neighbor interaction present in CaV_4O_9 .

OAS acknowledges helpful conversations with A. V. Chubukov. Two of us (DIK and RRPS) would like to thank the Gordon Godfrey Foundation for support at the University of New South Wales, where part of this work was done. OAS and RRPS are supported in part by NSF grant number DMR-9318537. DIK was supported in part by FOM, the Netherlands.

(1983).

- [16] M. C. Cross, D. S. Fisher, *Phys. Rev. B* **19**, 402 (1979).
- [17] L. N. Bulaevskii, A. I. Buzdin, and D. I. Khomskii, *Solid State Communications* **27**, 5 (1978).

FIG. 1. Lattice structure of CaV_4O_9 . Three types of exchange bonds are indicated by thick lines. The pattern of lattice distortion is shown schematically by thin dashed lines.

FIG. 2. Phase diagram of the model in linear approximation. Thick (thin) solid line denotes second (first) order phase transition. Regions of stability of dimer (plaquette) phase are shown by long (short) dashed lines.

-
- [1] S. Taniguchi *et al.*, *J. Phys. Soc. Jpn.* **64**, 2758 (1995).
 - [2] K. Ueda, H. Kontani, M. Sigrist, and P. A. Lee, *Phys. Rev. Lett.*, to appear (1996).
 - [3] N. Katoh and M. Imada, *J. Phys. Soc. Jpn* **64**, 4105 (1995).
 - [4] K. Sano and K. Takano, *cond-mat/9510160* (1995).
 - [5] M. Albrecht and F. Mila, *cond-mat/9511029* (1995).
 - [6] M. Troyer, H. Kontani, and K. Ueda, *cond-mat/9511074* (1995).
 - [7] S. Sachdev and R. N. Bhatt, *Phys. Rev. B* **41**, 9323 (1990).
 - [8] M. P. Gelfand, R. R. P. Singh, and D. A. Huse, *Phys. Rev. B* **40**, 10801 (1989).
 - [9] A. F. Barabanov, L. A. Maksimov, O. A. Starykh, and G. V. Uimin, *J. Phys.: Cond. Matter* **2**, 8925 (1990); A. F. Barabanov, L. A. Maksimov, and O. A. Starykh, *Int. J. Mod. Phys. B* **4**, 2319 (1990).
 - [10] V. I. Belinicher and L. V. Popovich, *Int. J. Mod. Phys. B* **8**, 2203 (1994).
 - [11] A. V. Chubukov and Th. Jolicoeur, *Phys. Rev. B* **44**, 12050 (1991); A. V. Chubukov and D. K. Morr, *ibid.* **52**, 3521 (1995).
 - [12] small deviation of the first order transition line from the crossing point of two instability lines is an artifact of the linear approximation and can be considered as a ‘systematic error bar’ put on this line.
 - [13] E. Shender, *Sov. Phys. JETP* **56**, 178 (1982)
 - [14] W. Harrison, *Electronic Structure and Properties of Solids*, Freeman, San Francisco (1980).
 - [15] J. W. Bray *et al.*, in *Extended linear chain compounds*, Vol. 3, 353, edited by J. S. Miller, Plenum, New York

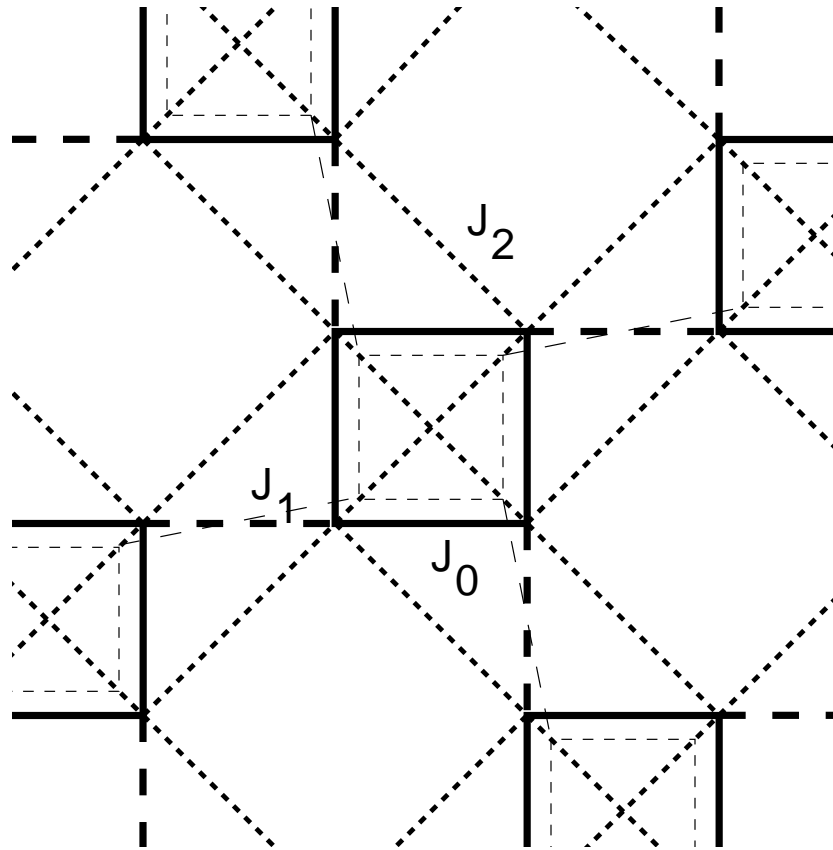


FIG.1 of Starykh et al.

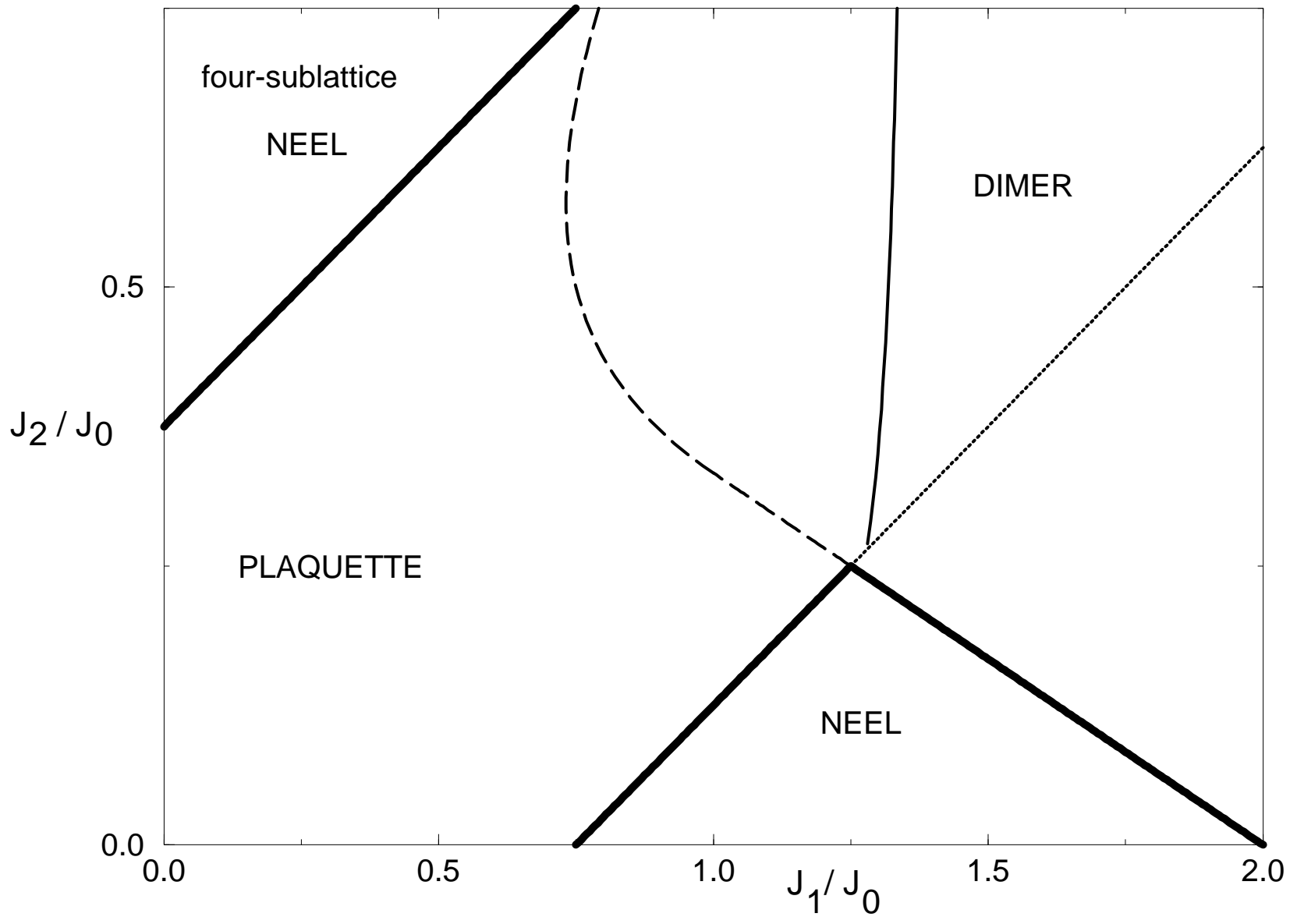


FIG.2 of Starykh et al.